From a Quasimolecular Band Insulator to a Relativistic Mott Insulator in t_{2g}^5 Systems with a Honeycomb Lattice Structure

Beom Hyun Kim,[1,2] Tomonori Shirakawa,[3] and Seiji Yunoki[1,2,3,4]
[1]Computational Condensed Matter Physics Laboratory, RIKEN, Wako, Saitama 351-0198, Japan
[2]Interdisciplinary Theoretical Science (iTHES) Research Group, RIKEN, Wako, Saitama 351-0198, Japan
[3]Computational Quantum Matter Research Team, RIKEN Center for Emergent Matter Science (CEMS), Wako, Saitama 351-0198, Japan
[4]Computational Materials Science Research Team, RIKEN Advanced Institute for Computational Science (AICS), Kobe, Hyogo 650-0047, Japan
(Received 18 June 2016; published 24 October 2016)

The t_{2g} orbitals of an edge-shared transition-metal oxide with a honeycomb lattice structure form dispersionless electronic bands when only hopping mediated by the edge-sharing oxygens is accessible. This is due to the formation of isolated quasimolecular orbitals (QMOs) in each hexagon, introduced recently by Mazin *et al.* [Phys. Rev. Lett. **109**, 197201 (2012)], which stabilizes a band insulating phase for t_{2g}^5 systems. However, with the help of the exact diagonalization method to treat the electron kinetics and correlations on an equal footing, we find that the QMOs are fragile against not only the spin-orbit coupling (SOC) but also the Coulomb repulsion. We show that the electronic phase of t_{2g}^5 systems can vary from a quasimolecular band insulator to a relativistic $J_{\rm eff} = 1/2$ Mott insulator with increasing the SOC as well as the Coulomb repulsion. The different electronic phases manifest themselves in electronic excitations observed in optical conductivity and resonant inelastic x-ray scattering. Based on our calculations, we assert that the currently known Ru^{3+} and Ir^{4+} based honeycomb systems are far from the quasimolecular band insulator but rather the relativistic Mott insulator.

DOI: 10.1103/PhysRevLett.117.187201

Introduction.—Physical properties of $4d$ and $5d$ transition metal (TM) compounds with nominally less than six d electrons are determined by the t_{2g} manifold because of a strong cubic crystal field. A strong spin-orbit coupling (SOC) causes t_{2g} orbitals to split into effective total angular momenta $j_{\rm eff} = 1/2$ and $3/2$. The relativistic electronic feature in these TM compounds has drawn much attention recently as exotic electronic, magnetic, and topological phases have been expected, including a $J_{\rm eff} = 1/2$ Mott insulator [1–5], superconductivity [6,7], topological insulator [8,9], Weyl semimetal [10,11], and spin liquid [12,13]. Among them, the research on t_{2g}^5 systems forming a honeycomb lattice structure with edge-sharing ligands has been triggered by the possibility of a nontrivial topological phase [14,15] or a Kitaev-type spin liquid [16–18], attributed to their unique hopping geometry. However, the existing compounds such as Na_2IrO_3 [19–22], Li_2IrO_3 [23], Li_2RhO_3 [24], and α-$RuCl_3$ [25–27], have turned out to be magnetic insulators with a long-range antiferromagnetic (AFM) or glassy-spin order.

In order to understand the electronic and magnetic structures of these compounds with t_{2g}^5 configuration, two distinct points of view, i.e., Mott- and Slater-type pictures, have been proposed. In the Mott picture, the Coulomb repulsion opens the gap of the relativistic $j_{\rm eff} = 1/2$ based band and the superexchange interaction between the relativistic isospins stabilizes the AFM order [28–33]. This strong coupling approach can successfully elucidate the observed excitations in the optical conductivity (OC) and resonant inelastic x-ray scattering (RIXS) for Na_2IrO_3 [31]. However, there has been still debate on the origin of the zigzag AFM order in Na_2IrO_3 [34,35]. In contrast, the Slater picture focuses on the itinerant nature of t_{2g} bands and treats the Coulomb interactions perturbatively. This weak coupling approach naturally explains the zigzag AFM order with a concomitantly induced band gap [36–39]. However, it is difficult to fully describe the observed excitations in the OC and RIXS for Na_2IrO_3 [40–42]. Because the hopping integral, Coulomb repulsion, and SOC are of similar energy scale, either of these two opposite pictures cannot be ruled out.

As the electron hoppings between the adjacent TMs via the two edge-sharing ligands are highly orbital dependent [43], the electron motion is confined within a single hexagon formed by six TMs. This has led to the notion of the quasimolecular orbital (QMO) formation [36], where each t_{2g} orbital of a TM participates in the formation of QMO at one of the three different hexagons around the TM. Therefore, when the SOC and Coulomb repulsion are both small, the ground state for t_{2g}^5 systems is a band insulator with a strong QMO character. However, when the SOC is strong, the QMOs are no longer well defined because the SOC induces an effective hopping between neighboring QMOs. In this limit, the local relativistic $j_{\rm eff}$ orbitals are

instead expected to play a dominant role in characterizing the electronic and magnetic structures.

In this Letter, by considering a minimal microscopic model which captures both extreme limits, we examine the ground state phase diagram for t_{2g}^5 electron configuration with the help of the numerically exact diagonalization method. We show that not only the SOC but also the Coulomb repulsion induces a crossover of the ground state with the strong QMO to relativistic $j_{\rm eff}$ orbital character. Concomitantly, the nature of the emerging electronic state varies from a quasimolecular band insulator to a relativistic $J_{\rm eff} = 1/2$ Mott insulator. The different electronic states are manifested in distinct behaviors of excitations, directly observed in OC and RIXS experiments. Our analysis concludes that the currently known Ru^{3+} and Ir^{4+} based systems are both far from the quasimolecular band insulator but they are rather the relativistic Mott insulator.

Noninteracting limit.—Without the SOC, the QMOs are the exact eigenstates with b_{1u}, e_{1g}, e_{2u}, and a_{1g} symmetries, the eigenenergies being $-2t$, $-t$, t, and $2t$ (t: hopping between adjacent TMs), respectively [43], and they form dispersionless bands. However, as shown in Fig. 1(a), once the SOC λ is finite, the double degeneracy of e_{1g} and e_{2u} symmetries is lifted and the QMOs are split in total into six Kramer's doublet bands with finite dispersion. With further increasing λ, the highest two bands as well as the lowest four bands come close in energy but the energy splitting between these two manifolds becomes larger, smoothly connecting to the $j_{\rm eff} = 1/2$ and $3/2$ based bands [see Fig. 1(b)]. Thus, as λ increases, an insulating gap of t_{2g}^5 systems for $t > 0$ gradually decreases with continuous change of hole character from a_{1g} to $j_{\rm eff} = 1/2$.

Correlation effect.—Let us now explore the effect of electron correlations by considering a three-band Hubbard model on a periodic six-site cluster for electron density $n = 5$

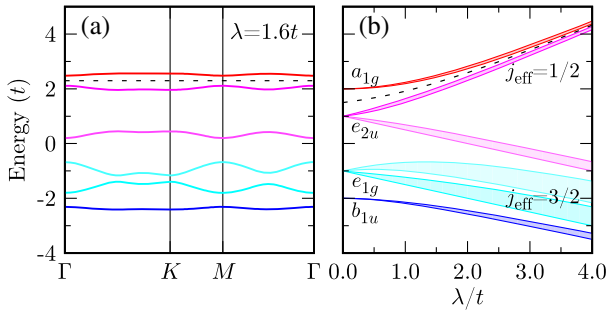

FIG. 1. (a) Noninteracting band dispersion with the hopping $t(>0)$ mediated by edge-sharing ligands for the SOC $\lambda = 1.6t$. Each band is doubly degenerate (Kramer's doublet). (b) Energy splitting of the noninteracting bands as a function of λ. Shaded region represents the band width of each band. a_{1g}, e_{2u}, e_{1g}, and b_{1u} refer to the symmetries of the quasimolecular bands when $\lambda = 0$. Dotted lines in (a) and (b) denote the Fermi energy for t_{2g}^5 systems.

[43] with Lanczos exact diagonalization method [47,48], which allows us to treat the electron kinetics inducing the QMO formation and the electron correlations on an equal footing, thus clearly going beyond the previous study [31]. We first examine the ground state as functions of the intra-orbital Coulomb repulsion U, Hund's coupling $J_{\rm H}$, and λ, and check the stability of the QMO state. For this purpose, we calculate the hole density $\bar{n}_{a_{1g}}$ of the a_{1g} quasimolecular band at the Γ point, which is exactly one for the pure QMO state [43]. Figure 2(a) shows the result of $\bar{n}_{a_{1g}}$ for $J_{\rm H} = 0$ with varying U and λ. It clearly demonstrates that λ and U are both destructive perturbations to the QMOs. As already pointed out in Ref. [38], the strong SOC mixes the three t_{2g} orbitals at each site, which gives rise to a finite overlap between the QMOs in neighboring hexagons, and thus it is unfavorable to the QMO formation. More interestingly, we find here in Fig. 2(a) that the Coulomb repulsion is also adequate for destroying the QMO state. This is understood because the Coulomb interactions promote the scattering among electrons bounded in adjacent hexagons.

The ground state is described by a direct product of local states with not only d^5 electron configuration but also other configurations such as d^4 and d^6. Therefore, the ground state is sensitive to the local multiplet structures of these electron configurations. According to the multiplet theory, the Hund's coupling $J_{\rm H}$ always brings about additional splitting of the d^4 multiplet hierarchy [43]. It is thus easily conjectured that $J_{\rm H}$ also plays a role in the QMO formation. Figure 2(b) well represents the effect of $J_{\rm H}$ on the QMO state. In finite $J_{\rm H}$, the region with the strong QMO character shrinks with somewhat smaller $\bar{n}_{a_{1g}}$ and the crossover boundary becomes sharper.

In the whole parameter region of Fig. 2, the ground state is insulating. However, the insulating nature is expected to vary from a band insulator to a Mott insulator across the boundary where the QMO character is abruptly lost. To verify this conjecture, we calculate the excitation spectrum $\Lambda_{1/2}(\omega)$ of a doublon-holon pair formed in the $j_{\rm eff} = 1/2$ orbitals at neighboring sites [43], excitations schematically

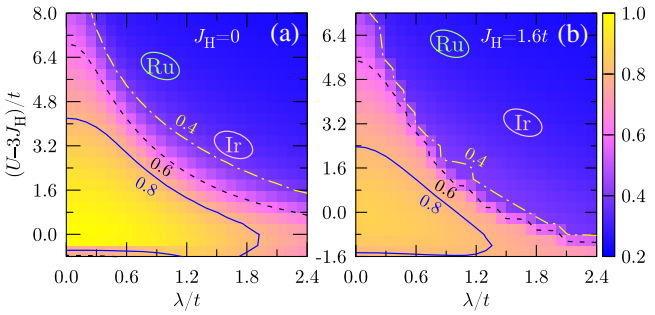

FIG. 2. The hole density $\bar{n}_{a_{1g}}$ of the a_{1g} quasimolecular band at the Γ point as functions of U and λ for (a) $J_{\rm H} = 0$ and (b) $J_{\rm H} = 1.6t$. Note that $\bar{n}_{a_{1g}} = 1$ for the pure QMO state. The loci of Ru^{3+} and Ir^{4+} based $4d$ and $5d$ transition-metal compounds are also indicated.

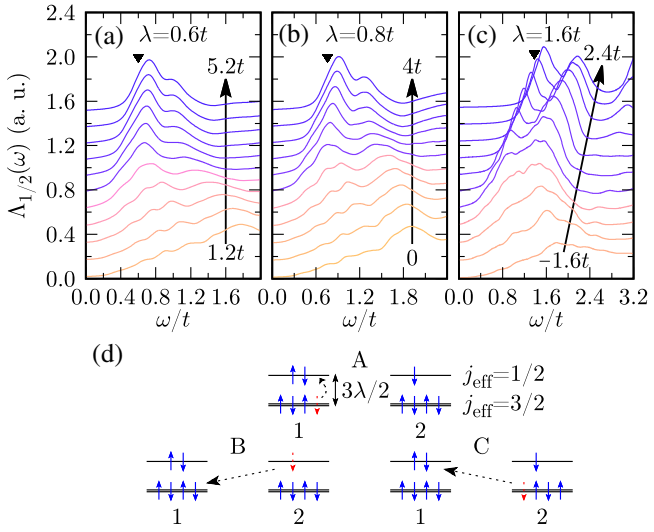

FIG. 3. (a)–(c): Excitation spectrum $\Lambda_{1/2}(\omega)$ of a doublon-holon pair formed in the neighboring $j_{\mathrm{eff}} = 1/2$ orbitals for (a) $\lambda = 0.6t$, (b) $0.8t$, and (c) $1.6t$ with different $U - 3J_{\mathrm{H}}$ values. $U - 3J_{\mathrm{H}}$ varies from (a) $1.2t$ to $5.2t$, (b) 0 to $4t$, and (c) $-1.6t$ to $2.4t$ with the same increment of $0.4t$. Solid triangles indicate peak positions of the excitonlike excitations in the RIXS spectrum for $U - 3J_{\mathrm{H}} = 5.2t$ (a), $4t$ (b), and $2t$ (c). We set $J_{\mathrm{H}} = 1.6t$ and different line colors correspond to the values of $\bar{n}_{a_{1g}}$ shown in Fig. 2(b). (d) Schematic energy diagrams of three relevant electron-hole excitations. Blue solid and red dotted arrows refer to electron and hole, respectively, and up and down arrows denote Kramer's doublet with positive (up arrow) and negative (down arrow) eigenvalues of j^z_{eff}. "1" and "2" indicate two neighboring TM sites.

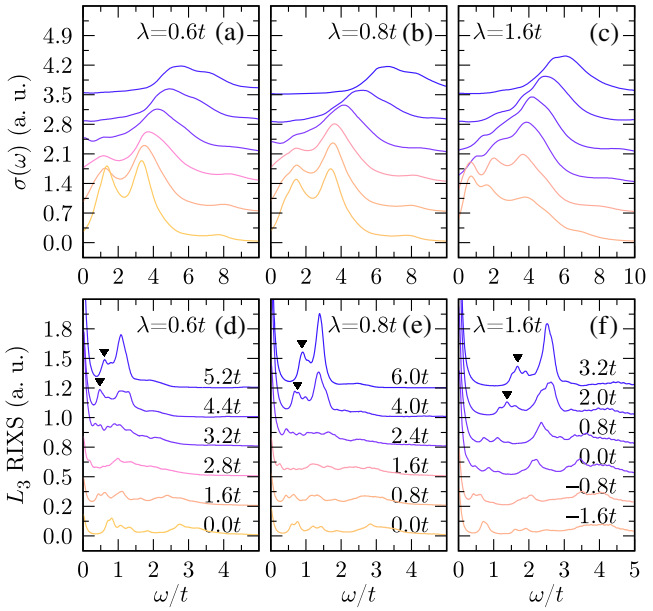

FIG. 4. (a)–(c) OC $\sigma(\omega)$ and (d)–(f) L_3-edge RIXS spectrum at wave number $\mathbf{q} = 0$ for $\lambda = 0.6t$ [(a) and (d)], $0.8t$ [(b) and (e)], and $1.6t$ [(c) and (f)] with various $U - 3J_{\mathrm{H}}$ values indicated in the figures. We set $J_{\mathrm{H}} = 1.6t$ and different line colors correspond to the values of $\bar{n}_{a_{1g}}$ shown in Fig. 2(b). The excitonlike excitations in the RIXS spectrum are indicated by solid triangles in (d)–(f).

shown in B of Fig. 3(d), which directly reflects the charge gap structure. As shown in Figs. 3(a)–3(c), the U dependence of $\Lambda_{1/2}(\omega)$ is qualitatively different across the crossover boundary. Below the boundary where the QMO character is strong, the low energy excitations shift downward in spite of increasing U, implying that an insulating gap evidently decreases with increasing electron repulsion. In contrast, above the boundary where the QMO character is lost, the clear increase of the lowest peak position is manifested with increasing U, indicating the increase of the gap as in a Mott insulator. The similar feature is also found when λ is increased with fixed U and J_{H} [43]. These results support the conjecture that the insulating nature changes across the crossover boundary. The conjecture is further supported by other excitation spectra shown below.

OC and RIXS spectra.—The Kubo formula and the continued fraction method are exploited to investigate the OC and L_3-edge RIXS spectra [43]. Figure 4 summarizes the results for $\lambda = 0.6t$, $0.8t$, and $1.6t$ with $J_{\mathrm{H}} = 1.6t$. Note that the QMO character suddenly diminishes at $U - 3J_{\mathrm{H}} \sim 3t$ for $\lambda = 0.6t$, $2t$ for $0.8t$, and 0 for $1.6t$, as shown in Fig. 2(b). The abrupt change of the electronic characteristics is reflected in these excitation spectra.

When the QMO character is strong with large $\bar{n}_{a_{1g}}$, the OC exhibits a two-peak structure for $\lambda = 0.6t$ and $0.8t$, and a three-peak structure for $\lambda = 1.6t$. The lower (higher) peak in the OC is attributed to the transition between the a_{1g} and e_{2u} (e_{1g}) quasimolecular bands whose energies are around t ($3t$) (see Fig. 1). The large splitting of the e_{2u} bands for the strong SOC can give an additional splitting to the lower peak in the OC. The RIXS spectrum also shows the similar peak structures near the similar excitation energies. Consequently, the excitations can be interpreted on the basis of the single-particle picture. Therefore, a strong band insulating character is predominant in this region.

In the region where the QMO character is degraded, the OC shows a one-peak structure and the peak position monotonically increases with U, while the RIXS spectra exhibits the dominant peak around $3\lambda/2$ in addition to an almost zero energy peak due to the magnetic excitation. These features can be well understood as on-site or intersite electron-hole excitations in the local relativistic j_{eff} orbitals. As shown in B and C of Fig. 3(d), two types of intersite electron-hole excitations can play a role in the OC. However, the edge-shared geometry suppresses the contribution of type B electron-hole excitation simply because the hopping between the neighboring $j_{\mathrm{eff}} = 1/2$ orbitals is zero [49]. Hence, only type C electron-hole excitation gives the dominant contribution to form the one-peaklike structure at excitation energy $\omega \approx U - 3J_{\mathrm{H}} + 3\lambda/2$. In the RIXS spectrum, an on-site electron-hole excitation indicated in A of Fig. 3(d), i.e., a local d-d transition between the $j_{\mathrm{eff}} = 3/2$ and $1/2$ orbitals, can give a dominant intensity at $\omega \approx 3\lambda/2$. Thus, both OC and RIXS spectra in this region

can be interpreted in terms of the relativistic Mott insulating picture.

In the relativistic Mott insulating limit, the RIXS spectrum shows an additional peak below the local d-d excitation ($\approx 3\lambda/2$) and above the almost zero energy magnetic peak, which is marked by triangles in Figs. 4(d)–4(f). Indeed, this peak has been observed in Na_2IrO_3 and the origin is attributed to the exciton formation induced by the intersite electron correlations [29]. However, the consecutive theoretical study based on the strong coupling model calculations has shown that this excitonlike peak appears even without considering the intersite electron correlations when the intersite migration of electrons from the $j_{\rm eff} = 1/2$ to $3/2$ orbitals [B of Fig. 3(d)] follows the local d-d transition [A of Fig. 3(d)], resulting in the intersite electron-hole excitation between the $j_{\rm eff} = 1/2$ orbitals [31]. As shown in Figs. 3(a)–3(c), the excitation spectrum $\Lambda_{1/2}(\omega)$ of a doublon-holon pair in the $j_{\rm eff} = 1/2$ orbitals also yields the obvious spectral weight in the vicinity of the excitonlike RIXS excitation energy, implying that these excitations are due to the same origin. In addition, the monotonic increase of the excitonlike peak position in the RIXS spectrum with U is also consistent with $\Lambda_{1/2}(\omega)$. We also find that the intensity of the excitonlike RIXS peak depends strongly on momentum [43], which is in good agreement with the experiments [29]. Thus, it is reasonable to infer that the origin of the excitonlike peak near the edge of local d-d excitation in the RIXS is due to the combined excitations of two different types (A and B).

Ir^{4+} and Ru^{3+} based systems.—A typical SOC is known to be 0.4–0.5 eV for $5d$ systems and 0.1–0.2 eV for $4d$ systems [50,51]. Recent theoretical studies have estimated that $t \approx 0.27$ eV for the most studied Ir^{4+} system Na_2IrO_3 [36,38,52], and $t \approx 0.11$ eV [33] and 0.16 eV [53] for α-$RuCl_3$ (Ru^{3+}), both of which are much smaller than that for Ir^{4+} systems. U and $J_{\rm H}$, however, are not easy to be determined because the full screening effect of electron correlations is hardly treated. One useful expedient is to extract them from the OC measurement.

Since the dominant optical peak appears near $U - 3J_{\rm H} + 3\lambda/2$, we can estimate $U - 3J_{\rm H} \sim 0.8$–1.0 eV for Na_2IrO_3 based on the existing OC data, which exhibit a one-peak structure around 1.6 eV [28,30]. Assuming $U - 3J_{\rm H} = 3.2t$ (≈ 0.86 eV), our results for the OC and RIXS spectra in Figs. 4(c) and 4(f) are both indeed in good quantitative agreement with the experiments [28–30], except for a double-peak structure around 0.7 eV ($\approx 2.6t$) observed in the RIXS experiment, instead of a single peak found in Fig. 4(f). Here, our calculations assume the cubic crystal field. However, the crystal structure of Na_2IrO_3 is known to display the additional trigonal distortion [54], thus significantly departing from the ideal IrO_6 octahedra [21]. This additional distortion can mix the relativistic $j_{\rm eff} = 1/2$ and $3/2$ orbitals, and lead to the splitting of the dominant RIXS peak of the local d-d transition into multiple subpeaks [55,56]. Indeed, we find that the single peak found in Fig. 4(f) is split into two (or multiple) subpeaks in the presence of the trigonal distortion [43] (see also Refs. [29,31]). Therefore, we can conclude that the electronic state of Na_2IrO_3 is far from the QMO limit and is located in the relativistic Mott insulating region, as indicated in Fig. 2.

The recent optical absorption experiments for α-$RuCl_3$ have found a dominant peak around 1.2 eV as well as a small additional peak near 0.3 eV [32,57]. The photoemission spectroscopy measurement has also observed a large gap about 1.2 eV [58]. Thus, $U - 3J_{\rm H}$ for α-$RuCl_3$ is estimated to be about 0.9–1.1 eV. Adopting $t = 0.16$ eV, our result for $U - 3J_{\rm H} = 6t$ (≈ 0.96 eV) and $\lambda = 0.8t$ (≈ 0.13 eV) in Fig. 4(b) also exhibits the dominant peak near 1.1 eV ($\approx 6.9t$). Although no experimental RIXS spectrum has been reported yet, the recent neutron scattering measurement on α-$RuCl_3$ observed an inelastic peak near 195 meV and estimated that $\lambda \approx 130$ meV [59]. This observation is consistent with a dominant RIXS peak around $1.4t$ (≈ 0.22 eV) for $U - 3J_{\rm H} = 6t$ in Fig. 4(e). Therefore, we expect that α-$RuCl_3$ is located also in the QMO poor region, as indicated in Fig. 2.

It should be noted, however, that the OC for $U - 3J_{\rm H} = 6t$ in Fig. 4(b) fails to yield the low-energy peak near 0.3 eV observed experimentally in α-$RuCl_3$. This can be explained by considering an additional direct d-d hopping t' between neighboring sites, estimated as large as -0.23 eV in Ref. [33] and -0.15 eV in Ref. [53]. As discussed in the Supplemental Material [43], the low-energy peak attributed to the local d-d transition [A in Fig. 3(d)] can emerge because the forbidden optical transition among the $j_{\rm eff} = 1/2$ bands without the direct hopping t' can now be accessed in the presence of t' [60]. The experimental fact that the intensity of the low-energy peak near 0.3 eV is much weaker than that of the dominant peak around 1.2 eV suggests that the strength of t' is not as large as the theoretical estimation [43].

Conclusion.—Based on the numerically exact diagonalization analyses of the three-band Hubbard model, we have shown that the ground state of the t_{2g}^5 system with the honeycomb lattice structure can be transferred from the quasimolecular band insulator to the relativistic Mott insulator with increasing λ as well as U when the QMOs are disturbed and eventually replaced by the local relativistic $j_{\rm eff}$ orbitals. We have demonstrated that the different electronic nature of these insulators is manifested in the electronic excitations observed in OC and RIXS. Comparing our results with experiments, we predict that not only Na_2IrO_3 with strong SOC but also α-$RuCl_3$ with moderate SOC is the relativistic Mott insulator. This deserves further experimental confirmation, especially for α-$RuCl_3$ where we expect the excitonlike excitation near the edge of the local d-d excitation in the RIXS spectrum.

The numerical computations have been performed with the RIKEN supercomputer system (HOKUSAI GreatWave). This work has been supported by Grant-in-Aid for Scientific Research from MEXT Japan under Grant No. 25287096 and also by RIKEN iTHES Project and Molecular Systems.

[1] B. J. Kim, H. Jin, S. J. Moon, J.-Y. Kim, B.-G. Park, C. S. Leem, J. Yu, T. W. Noh, C. Kim, S.-J. Oh, J.-H. Park, V. Durairaj, G. Cao, and E. Rotenberg, Phys. Rev. Lett. **101**, 076402 (2008).
[2] B. J. Kim, H. Ohsumi, T. Komesu, S. Sakai, T. Morita, H. Takagi, and T. Arima, Science **323**, 1329 (2009).
[3] G. Jackeli and G. Khaliullin, Phys. Rev. Lett. **102**, 017205 (2009).
[4] H. Watanabe, T. Shirakawa, and S. Yunoki, Phys. Rev. Lett. **105**, 216410 (2010).
[5] C. Martins, M. Aichhorn, L. Vaugier, and S. Biermann, Phys. Rev. Lett. **107**, 266404 (2011).
[6] F. Wang and T. Senthil, Phys. Rev. Lett. **106**, 136402 (2011).
[7] H. Watanabe, T. Shirakawa, and S. Yunoki, Phys. Rev. Lett. **110**, 027002 (2013).
[8] D. Pesin and L. Balents, Nat. Phys. **6**, 376 (2010).
[9] B.-J. Yang and Y. B. Kim, Phys. Rev. B **82**, 085111 (2010).
[10] W. Witczak-Krempa and Y. B. Kim, Phys. Rev. B **85**, 045124 (2012).
[11] A. Go, W. Witczak-Krempa, G. S. Jeon, K. Park, and Y. B. Kim, Phys. Rev. Lett. **109**, 066401 (2012).
[12] Y. Okamoto, M. Nohara, H. Aruga-Katori, and H. Takagi, Phys. Rev. Lett. **99**, 137207 (2007).
[13] Y. Singh, Y. Tokiwa, J. Dong, and P. Gegenwart, Phys. Rev. B **88**, 220413(R) (2013).
[14] A. Shitade, H. Katsura, J. Kuneš, X.-L. Qi, S.-C. Zhang, and N. Nagaosa, Phys. Rev. Lett. **102**, 256403 (2009).
[15] C. H. Kim, H. S. Kim, H. Jeong, H. Jin, and J. Yu, Phys. Rev. Lett. **108**, 106401 (2012).
[16] J. Chaloupka, G. Jackeli, and G. Khaliullin, Phys. Rev. Lett. **105**, 027204 (2010).
[17] H.-C. Jiang, Z.-C. Gu, X.-L. Qi, and S. Trebst, Phys. Rev. B **83**, 245104 (2011).
[18] J. Reuther, R. Thomale, and S. Trebst, Phys. Rev. B **84**, 100406(R) (2011).
[19] Y. Singh and P. Gegenwart, Phys. Rev. B **82**, 064412 (2010).
[20] X. Liu, T. Berlijn, W.-G. Yin, W. Ku, A. Tsvelik, Y.-J. Kim, H. Gretarsson, Y. Singh, P. Gegenwart, and J. P. Hill, Phys. Rev. B **83**, 220403(R) (2011).
[21] S. K. Choi, R. Coldea, A. N. Kolmogorov, T. Lancaster, I. I. Mazin, S. J. Blundell, P. G. Radaelli, Y. Singh, P. Gegenwart, K. R. Choi, S.-W. Cheong, P. J. Baker, C. Stock, and J. Taylor, Phys. Rev. Lett. **108**, 127204 (2012).
[22] F. Ye, S. Chi, H. Cao, B. C. Chakoumakos, J. A. Fernandez-Baca, R. Custelcean, T. F. Qi, O. B. Korneta, and G. Cao, Phys. Rev. B **85**, 180403(R) (2012).
[23] Y. Singh, S. Manni, J. Reuther, T. Berlijn, R. Thomale, W. Ku, S. Trebst, and P. Gegenwart, Phys. Rev. Lett. **108**, 127203 (2012).
[24] Y. Luo, C. Cao, B. Si, Y. Li, J. Bao, H. Guo, X. Yang, C. Shen, C. Feng, J. Dai, G. Cao, and Z.-a. Xu, Phys. Rev. B **87**, 161121(R) (2013).
[25] J. A. Sears, M. Songvilay, K. W. Plumb, J. P. Clancy, Y. Qiu, Y. Zhao, D. Parshall, and Y.-J. Kim, Phys. Rev. B **91**, 144420 (2015).
[26] M. Majumder, M. Schmidt, H. Rosner, A. A. Tsirlin, H. Yasuoka, and M. Baenitz, Phys. Rev. B **91**, 180401(R) (2015).
[27] R. D. Johnson, S. C. Williams, A. A. Haghighirad, J. Singleton, V. Zapf, P. Manuel, I. I. Mazin, Y. Li, H. O. Jeschke, R. Valentí, and R. Coldea, Phys. Rev. B **92**, 235119 (2015).
[28] R. Comin, G. Levy, B. Ludbrook, Z.-H. Zhu, C. N. Veenstra, J. A. Rosen, Y. Singh, P. Gegenwart, D. Stricker, J. N. Hancock, D. van der Marel, I. S. Elfimov, and A. Damascelli, Phys. Rev. Lett. **109**, 266406 (2012).
[29] H. Gretarsson, J. P. Clancy, X. Liu, J. P. Hill, E. Bozin, Y. Singh, S. Manni, P. Gegenwart, J. Kim, A. H. Said, D. Casa, T. Gog, M. H. Upton, H.-S. Kim, J. Yu, V. M. Katukuri, L. Hozoi, J. van den Brink, and Y.-J. Kim, Phys. Rev. Lett. **110**, 076402 (2013).
[30] C. H. Sohn, H.-S. Kim, T. F. Qi, D. W. Jeong, H. J. Park, H. K. Yoo, H. H. Kim, J.-Y. Kim, T. D. Kang, D.-Y. Cho, G. Cao, J. Yu, S. J. Moon, and T. W. Noh, Phys. Rev. B **88**, 085125 (2013).
[31] B. H. Kim, G. Khaliullin, and B. I. Min, Phys. Rev. B **89**, 081109(R) (2014).
[32] K. W. Plumb, J. P. Clancy, L. J. Sandilands, V. V. Shankar, Y. F. Hu, K. S. Burch, H.-Y. Kee, and Y.-J. Kim, Phys. Rev. B **90**, 041112(R) (2014).
[33] H.-S. Kim, Vijay Shankar V., A. Catuneanu, and H.-Y. Kee, Phys. Rev. B **91**, 241110(R) (2015).
[34] I. Kimchi and Y.-Z. You, Phys. Rev. B **84**, 180407(R) (2011).
[35] J. Chaloupka, G. Jackeli, and G. Khaliullin, Phys. Rev. Lett. **110**, 097204 (2013).
[36] I. I. Mazin, H. O. Jeschke, K. Foyevtsova, R. Valentí, and D. I. Khomskii, Phys. Rev. Lett. **109**, 197201 (2012).
[37] I. I. Mazin, S. Manni, K. Foyevtsova, H. O. Jeschke, P. Gegenwart, and R. Valentí, Phys. Rev. B **88**, 035115 (2013).
[38] K. Foyevtsova, H. O. Jeschke, I. I. Mazin, D. I. Khomskii, and R. Valentí, Phys. Rev. B **88**, 035107 (2013).
[39] H.-J. Kim, J.-H. Lee, and J.-H. Cho, Sci. Rep. **4**, 5253 (2014).
[40] Y. Li, K. Foyevtsova, H. O. Jeschke, and R. Valentí, Phys. Rev. B **91**, 161101(R) (2015).
[41] M. Kim, B. H. Kim, and B. I. Min, Phys. Rev. B **93**, 195135 (2016).
[42] J.-i. Igarashi and T. Nagao, J. Phys. Condens. Matter **28**, 026006 (2016).
[43] See Supplemental Material at http://link.aps.org/supplemental/10.1103/PhysRevLett.117.187201, which also includes Refs. [44–46], for the detailed Hamiltonian, quasimolecular bands, cluster calculation of $\bar{n}_{a_{1g}}$, $\Lambda_{1/2}(\omega)$, OC and RIXS spectra, local multiplet structures, and the effect of the direct hopping on OC and RIXS spectra.
[44] J. Kanamori, Prog. Theor. Phys. **30**, 275 (1963).
[45] L. J. P. Ament, M. van Veenendaal, T. P. Devereaux, J. P. Hill, and J. van den Brink, Rev. Mod. Phys. **83**, 705 (2011).

[46] S. H. Chun, J.-W. Kim, J. Kim, H. Zheng, C. C. Stoumpos, C. D. Malliakas, J. F. Mitchell, K. Mehlawat, Y. Singh, Y. Choi, T. Gog, A. Al-Zein, M. M. Sala, M. Krisch, J. Chaloupka, G. Jackeli, G. Khaliullin, and B. J. Kim, Nat. Phys. **11**, 462 (2015).

[47] R. B. Morgan and D. S. Scott, SIAM J. Sci. Comput. **14**, 585 (1993).

[48] E. Dagotto, Rev. Mod. Phys. **66**, 763 (1994).

[49] Let t and t' be the nearest neighbor hoppings between YZ and ZX orbitals, and between XY orbitals, respectively, along the XY direction. One can show that the nearest neighbor hopping between $j_{\mathrm{eff}} = 1/2$ orbitals with the same isospin is $t'/3$. Therefore, there is no optical transition among the pure $j_{\mathrm{eff}} = 1/2$ bands when $t' = 0$.

[50] D. Dai, H. J. Xiang, and M.-H. Whangbo, J. Comput. Chem. **29**, 2187 (2008).

[51] J. P. Clancy, N. Chen, C. Y. Kim, W. F. Chen, K. W. Plumb, B. C. Jeon, T. W. Noh, and Y.-J. Kim, Phys. Rev. B **86**, 195131 (2012).

[52] Y. Yamaji, Y. Nomura, M. Kurita, R. Arita, and M. Imada, Phys. Rev. Lett. **113**, 107201 (2014).

[53] S. M. Winter, Y. Li, H. O. Jeschke, and R. Valentí, Phys. Rev. B **93**, 214431 (2016).

[54] The trigonal crystal field splitting among t_{2g} orbitals is estimated as large as 75 meV in Ref. [38].

[55] X. Liu, V. M. Katukuri, L. Hozoi, W.-G. Yin, M. P. M. Dean, M. H. Upton, J. Kim, D. Casa, A. Said, T. Gog, T. F. Qi, G. Cao, A. M. Tsvelik, J. van den Brink, and J. P. Hill, Phys. Rev. Lett. **109**, 157401 (2012).

[56] E. M. Plotnikova, M. Daghofer, J. van den Brink, and K. Wohlfeld, Phys. Rev. Lett. **116**, 106401 (2016).

[57] L. J. Sandilands, Y. Tian, A. A. Reijnders, H.-S. Kim, K. W. Plumb, Y.-J. Kim, H.-Y. Kee, and K. S. Burch, Phys. Rev. B **93**, 075144 (2016).

[58] A. Koitzsch, C. Habenicht, E. Müller, M. Knupfer, B. Büchner, H. C. Kandpal, J. van den Brink, D. Nowak, A. Isaeva, and Th. Doert, Phys. Rev. Lett. **117**, 126403 (2016).

[59] A. Banerjee, C. A. Bridges, J.-Q. Yan, A. A. Aczel, L. Li, M. B. Stone, G. E. Granroth, M. D. Lumsden, Y. Yiu, J. Knolle, S. Bhattacharjee, D. L. Kovrizhin, R. Moessner, D. A. Tennant, D. G. Mandrus, and S. E. Nagler, Nat. Mater. **15**, 733 (2016).

[60] In Ref. [57], the small low-energy peak near 0.3 eV is attributed to an optically forbidden local d-d transition from the t_{2g} bands to the e_g bands through electron-phonon coupling. However, our result supports that the pure electronic transition within the t_{2g} manifold can give rise to the low-energy optical excitations.